CrossMark

ORIGINAL ARTICLE

Hydrochemical and isotopic investigations as indicators of recharge processes of the Continental Intercalaire aquifer (eastern piedmont of Dahar, southern Tunisia)

Zahra Dhaoui[1] · Kamel Zouari[1] · Jean-Denis Taupin[2] · Rachid Farouni[3]

Abstract Groundwaters of the Continental Intercalaire sandstone formations at the eastern piedmont of Dahar (southern Tunisia), where they outcrop, were analysed to study the mineralization, the water origin and the current recharge process. Hydrochemical study shows that these waters present a spatial variability of chemical facies which is linked to the lithology of the host rock. The factors contributing to the mineralization are mainly the water–rock interaction in particular the dissolution of evaporitic minerals and the cation exchange reactions. Stable isotopes show an enrichment in $\delta^{18}O$ and $\delta^{2}H$ contents principally for piezometric levels closest to the surface, reflecting measures found in the current rainfall subject to a semi-arid to arid context. These results are coherent with those of ^{14}C and ^{3}H that allow the qualitative identification of a current recharge which could probably be supplied by the recent infiltration of waters in Wadis and by the direct infiltration of meteoric water through the local sandstone outcrops of the basin. This concerns in particular the well of Salem ben Salem Dabbabi, showing a content of 1.03 TU, and its static level is controlled by the Tataouine Wadi, indicating therefore an evident sign of recent recharge.

✉ Zahra Dhaoui
    zahra.dhaoui@gmail.com

    Kamel Zouari
    kamel.zouari@enis.rnu.tn

    Jean-Denis Taupin
    Jean-Denis.Taupin@univ-montp2.fr

    Rachid Farouni
    rachidfarouni@yahoo.fr

[1] Laboratory of Radio Analysis and Environment, Geology Department, National School of Engineers of Sfax, Route de Soukra, BP 1173, 3038 Sfax, Tunisia

[2] UMR 5569 Hydrosciences, Montpellier (IRD, CNRS, UM), BP 64501, 34394 Montpellier Cedex 5, France

[3] Commissariat Régional au Développement Agricole, 03 Rue Jamila Bouhired, 3200 Tataouine, Tunisia

Introduction

Groundwater resources are often the only sustainable water resources in arid and semi-arid regions. The CI aquifer (1 million km^2), one of the largest confined aquifers in the world, shared between Algeria (700.000 km^2), Tunisia (80.000 km^2) and Libya (250.000 km^2), constitutes the main groundwater resource in southern Tunisia. An increase in the number of this deep water table-equipped well is noticeable and constantly increasing. This intensive groundwater mobilization, although supplying the water needs in the different economic sectors (agriculture, drinking water, tourism, industry) with preponderance of the agricultural needs, seems to have regressive effects on the piezometric level, artesianism and springs flow rate but most likely on the water quality. In southern Tunisia, the CI aquifer covers mainly the regions of Tozeur, Kebili and the extreme south. The most important production takes place in the geothermal regions of Kebili (Nefzaoua) and Tozeur (Djerid) with, respectively, 1000 and 600 l/s (Kamel et al. 2007). The CI formations show changes in facies and thickness from the chains of Gafsa–Metlaoui to the north towards the Saharan platform to the south. In the Djerid region, the reservoir depth ranges between 1500 and 2400 m with a pressure varying from 60 m (well Nafta CI3) up to 200 m (well Hazoua CI) above the wellhead. The water temperature is

about 70 °C. Geothermal water is mainly used in agriculture, irrigation of oases and greenhouses. The transmissivity of the aquifer (Sidi Aich formation in the Djerid region) obtained from pumping tests varies from 0.8×10^{-3} to 4.5×10^{-3} m^2/s with a storage coefficient ranging between 0.2×10^{-4} and 1.4×10^{-4} (Mamou 1989). The dimensions of this aquifer and the nature of the hydrogeological issues justify the several devoted scientific studies (ERESS 1972; Ben Baccar 1982; Mamou 1990; Yahyaoui 1996; OSS 2003; Baba-Sy 2005; Petersen 2014). These reviews helped to make the essential knowledgeable elements to improve understanding of the CI aquifer hydrogeological functioning throughout the northern Sahara. In this study, we are particularly interested in the Continental Intercalaire recharge conditions, at the eastern piedmont of the Dahar uplands, which represents the only outcrop of this formation, dated of lower Cretaceous in southern Tunisia. The CI outcrops are mainly located on the boundaries of the basin, in the form of mountains such as the Algerian Atlas or Tunisian Dahar and in the form of plateau such as Tinhert (Busson 1967). It is mainly a confined aquifer that discharges in the Chotts region and the Gulf of Gabes in southern Tunisia (Guendouz et al. 2003).

With this significant increase in groundwater exploitation, the variability of the aquifer natural recharge is discussed. These deep aquifers, constituting huge groundwater reserves, recharged under humid periods during the Late Pleistocene (Guendouz et al. 1997) may currently be supplied under predominant arid and semi-arid conditions?

A geochemical approach based on the use of different environmental tracers has allowed to highlight different processes of the water mineralization. Stable isotopes of the water molecule (δ^{18}O and δ^2H) are considered as conservative tracers that indicate the groundwater origin and also the physical processes affecting water masses for instance evaporation, reservoirs mixing (Geyh 2000). With its properties and anthropogenic variability in relation to the atmosphere nuclear tests, the tritium (^{3}H), radioactive isotope of the water molecule with a 12.3 half life, was considered, between 1950 and 2000 as the simplest and the most common tracer to determine the age of groundwater with short residence time (Maduabuchi et al. 2006). Since the return to natural concentrations, it is rather used as an indicator of recent recharge.

Study area

The CI sandstone formations outcrop in the eastern piedmont of Dahar between the Djeffara plain to the East and the plateau of Dahar to the West (Fig. 1). These formations extend along 3770 km^2, between latitudes 31° 59′ and 33° 11′N and longitudes 10° 5′ and 10° 41′E. The region climate is arid to semi-arid with Saharan tendencies. Precipitations are characterized by their irregularities and

Fig. 1 Location and geological map of the study area
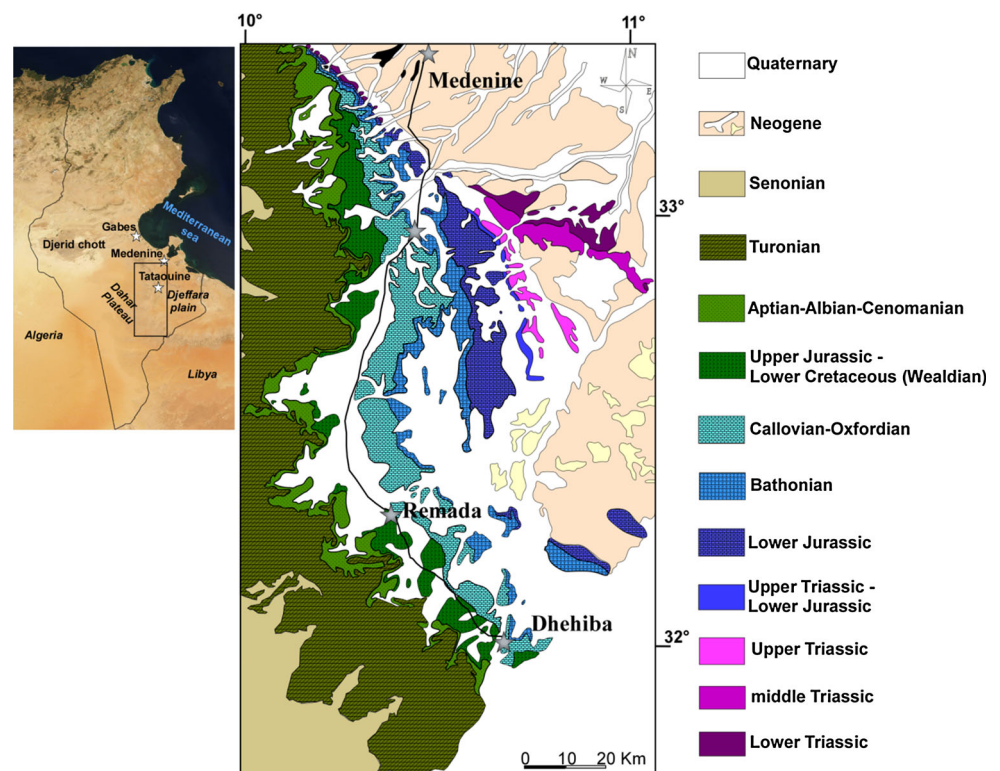
violence; they are usually brief and stormy favouring runoff (Yahyaoui 1996).

The rainfall data observation over 25 years (1987–1988 to 2013–2014) at Tataouine meteorological station (Tataouine CRDA) shows an average annual value of 108.5 mm/year with a minimum of 14.7 mm recorded in 2012–2013 and a maximum of 244.2 mm in 2010–2011. At Dehiba meteorological station (Dhibat CRA); the average annual rainfall data over a period of 18 years (1995–1996 to 2013–2014) is 78.9 mm/year with a minimum of 8.5 mm recorded in 2009–2010 and a maximum of 216 mm in 1995–1996. The rainy season in Tataouine as well as in Remada begins in September and ends in March.

The average temperature in this region is about 21 °C. The maximum temperature does not exceed 37.2 °C, and the minimum does not drop below 5 °C. In arid regions, evaporation and evapotranspiration are the major mechanisms of water loss. The mean potential evapotranspiration ranges around 1.700 mm year^{-1}.

Geology and hydrogeology

The CI is composed of clayey sands deposits from the lower Cretaceous and the Upper Jurassic-age. These deposits are divided in two groups and five formations: In ascending order, the group of Marbah el Asfer (Bir Miteur, Boulouha and Douiret formations) and the group of Ain El Guettar (Chenini and Oum ed Diab members) (Peybernès et al. 1985; Ben Ismail 1991; Barale and Ouaja 2002; Bodin et al. 2010). The detrital member of Marbah el Asfer consists of sandy and gypsified clays with some dolomitic intercalations and often clayey sands (Busson 1967). The most complete outcrops of this member are observed in the region of Marbah el Asfer western Tataouine. Its thickness is about 120 m. Towards the south, the sands of this formation become more abundant and coarse, with respect to clays and dolomite. Boreholes data show that this sandy series thickness decreases remarkably at Bir Zar area (115 km south-western Remada) and does not exceed 50 m.

Groundwaters of the CI aquifer in the eastern piedmont of Dahar are logged in the sandstone formations of the Marbah el Asfer representing the lower aquifer (Wealdian) and of Ain el Guettar constituting the upper aquifer (Albian). This bilayer aquifer system is separated by a clayey reference strata attributed to the Douiret formation dated of Lower Aptian (Ben Ismail 1991) which forms an impermeable screen where the two hydrogeological units are obviously separated. Indeed, the Douiret formation is composed of green clays rarely red with dolomitic beds. This formation outcrops widely in the Douiret area. Its average thickness is of 43 m. It is characterized by a lateral continuity and outcrops from the Oued el Khil locality in the north towards the south and the east in Algeria and Libya (Busson 1967; Bodin et al. 2010). From the north to the south, a lateral facies change resulting in an invasion of the Douiret formation basement with detrital elements has been demonstrated in outcrop as well as in subsurface. Nevertheless, the green clays remain the main constituents of this formation. The permeability through these clay deposits is about 10^{-7} m/s (Yahyaoui 1996). At the top of the Douiret formation, we distinguish the sandstone sequence of Ain el Guettar formation, which consists of friable to coarse-grained sandstone with clay and dolomitic intercalations in the locality of Ain el Guettar. This formation is limited to the top by dolomite and dolomitic clays with disappearance of detrital deposits (Yahyaoui 1996). The average transmissivity of the Albian water table in the Bir Amir region is about 44.10^{-3} m^2/s and about 4.10^{-3} m^2/s in the oriental Dahar (Yahyaoui 1996). In Chenini region, a constant level of stratified sandstone has been identified and assigned to Ain el Guettar formation; it represents the Chenini member which is overlain by the Oum ed Diab member sands (Burollet and Manderscheid 1965; Fanti et al. 2012).

The overlying carbonate successions of Cenomanian and Turonian are represented by the Zebbag formation (Rhadouane, Kerker and Gattar members) (Busson 1967; Ben Youssef et al. 1985; Bouaziz et al. 1988; Abdallah and Meister 1997; Robaszynski et al. 2010).

During the lower Cretaceous, tectonics have largely controlled deposition in the Tataouine basin and resulted in major variations in terms of subsidence and facies change. Overall, this basin is interpreted as a large tilted block controlled by east–west-oriented fault system (Underdown et al. 2007; Lazzez et al. 2008; Bodin et al. 2010; Raulin et al. 2011).

The geometry of the aquifer indicates that the flow direction of the CI water table is coming from Dahar outcrops towards the west and the south-west (Fig. 2). For the lower aquifer (Wealdian), only few piezometric data of shallow representative wells are available. These data indicate a static level between 15 and 40 m depth.

Methodology

Data for this study have been collected in the Tataouine basin along a 150-km-long, north–south-oriented section of the Dahar piedmont. This section covers the area between the localities of Bani Khedach in the north to Dehiba (approximately 43 km south-east of Remada) in the south (Fig. 3). A total of 29 samples were collected from the Tataouine basin. Samples were specified according to the classification shown in Table 1. Samples 1–22 were collected from the lower Wealdian aquifer,; boreholes 23–28 were sampled from the upper Albian aquifer. Sample 29 represents measurements taken at downstream and upstream El-Achouch spring located in Remada region.

Fig. 2 Hydrogeological cross section across Dahar cliff showing the flow direction of the CI groundwaters
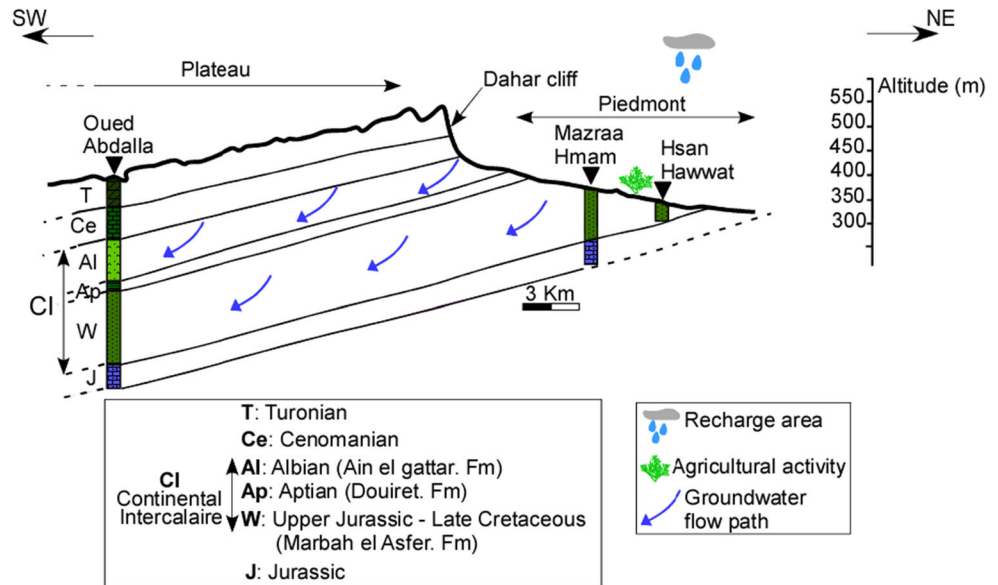
This spring represents the emergence of the Wealdian water table to the east of the Dahar cliff through Remada-Bahiret El Bibane fault. It is considered as a local outlet resulting in the interconnection between the lower Wealdian aquifer of the CI and the shallow aquifers of El Ouara plain towards the east of Remada (Teissier 1968).

The physico-chemical parameters, such as pH, temperature and electrical conductivity (EC), were performed in situ (Table 1). Chemical analysis and isotopic measurements (^{18}O, ^2H, ^3H) were determined in the Radio-Analysis and Environment Laboratory of the National School of Engineers of Sfax (Tunisia). Major elements (Na^+, Ca^{2+}, Mg^{2+}, K^+, Cl^-, SO_4^{2-}, HCO_3^- and NO_3^-) were analysed by ion liquid chromatography (ILC) equipped with columns IC-Pak TM CM/D for cations, using EDTA and nitric acid as eluent, and on a Metrohm chromatograph equipped with columns CI SUPER-SEP for anions using phthalic acid and acetonitrile as eluent. The CO_3^{2-} and HCO_3^- concentrations were analysed by titration using 0.1 N HCl acid. The ionic balance for all samples is within ±5 %. Stable isotope ratio ($^{18}O/^{16}O$ and $^2H/^1H$) analysis was performed using laser absorption spectrometry (LGR DLT 100) (Penna et al. 2010). Analyses are reported in per mil (‰) versus Vienna-Standard Mean Oceanic Water (V-SMOW). The analytical error is ±0.1 ‰ for $\delta^{18}O$, ±1 ‰ for Deuterium and ±0.3 TU for tritium.

Results and discussion

Physico-chemical parameters

CI groundwaters in the piedmont of Dahar show heterogeneous values of temperature, varying between 16 and 25.2 °C with an average of 20.5 °C close to the area mean annual air temperature which is around 21 °C. This parameter should be measured directly at the outflow because it is often influenced due to water pumping which may cause a prolonged contact and equilibrium with the atmospheric temperature (Huneau et al. 2011). In our case, the most discarded points with temperatures less than 19 °C or higher than 23 °C were sampled in January and June, respectively, therefore, subjected to an equilibrium with the atmospheric temperature during sampling. Measured pH values range from 7.07 to 8.36.

Shallow wells characterize groundwater from Marbah el Asfer formation (lower aquifer-Wealdian) with depth varying from 20.8 m (well No. 19) to 50 m (static water level between 15 and 40 m depth). These groundwaters are also managed by deep wells up to 160 m (well No. 4) revealing the confined part under Dahar cliff. However, groundwaters from Ain el Guettar formation (upper aquifer-Albian) are only exploited by deep wells with depth ranging from 125 to 150 m and static level varying from 37 to 125 m.

EC measurements vary between 1116 and 9372 µS/cm for groundwaters of the lower aquifer (Wealdian). For the upper aquifer (Albian), the measured EC varies from 1458 to 6400 µS/cm. Groundwater salinity, represented by the total dissolved salts (TDS) values, displays a wide range of variation from 780 (sample No. 21) to 8442 mg/l (sample No. 15) suggesting the occurrence of highly mineralized waters in the lower Wealdian aquifer. For the upper Albian aquifer, the TDS vary from 1075 (sample No. 24) to 4140 mg/l (sample No. 23). The lower EC values of groundwater flowing in the recharge area are explained by the permeability of the aquifer formation in the unsaturated zone which is essentially formed by sands and clayey sands.
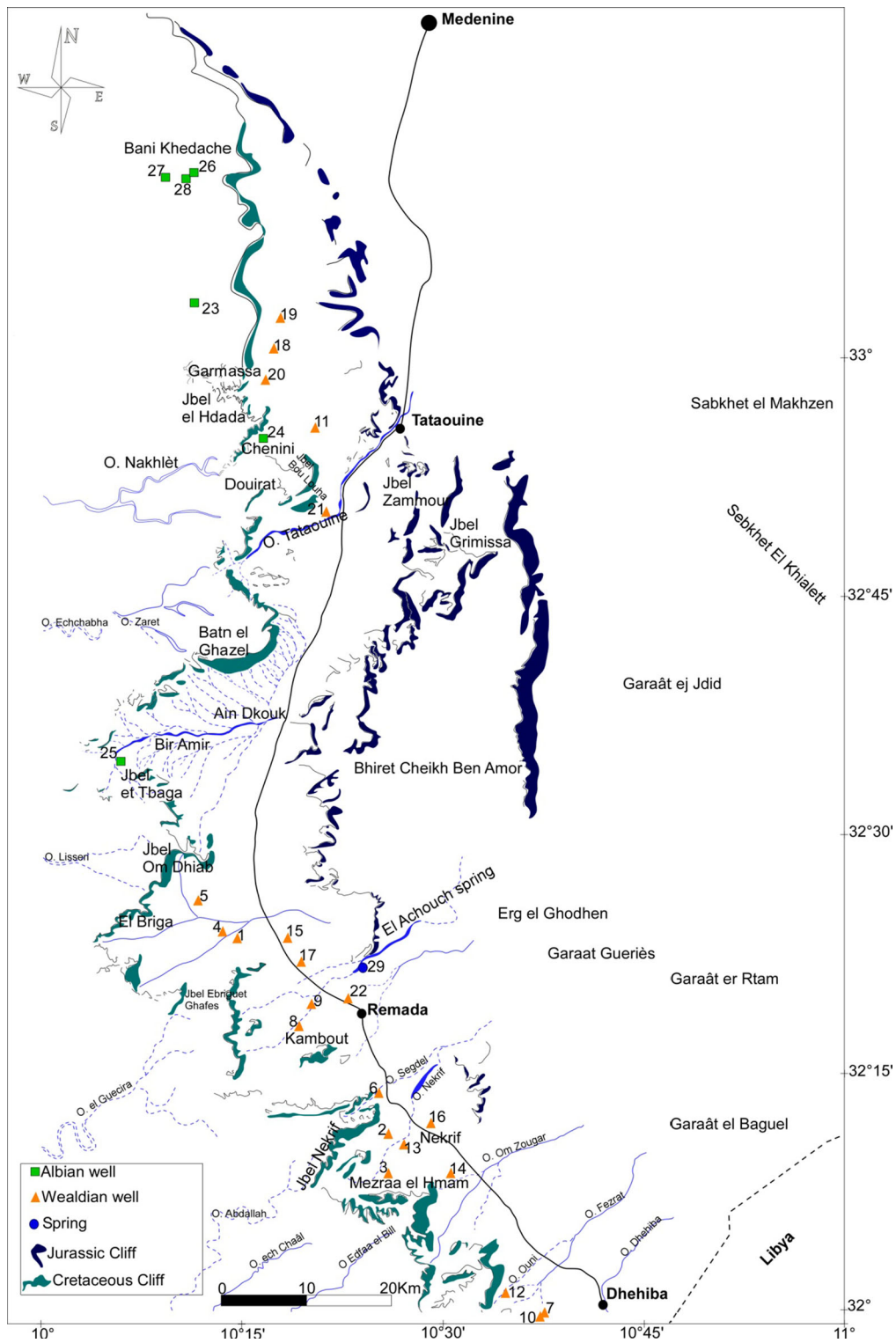
Fig. 3 Sampling map

Major elements geochemistry

The data plotted in Piper trilinear classification diagram show a large spatial variability of groundwater facies (Fig. 4). For the lower Wealdian aquifer, three chemically different groups are distinguished: Group 1, Na–Cl water type characterizing three shallow wells (No. 14, 15, 17) and 7 boreholes (No. 1, 2, 3, 8, 9, 10 and 12). The

Table 1 In situ measurements, hydrochemical and isotopic data of studied groundwaters

No.	Sample type	Altitude (m)	Total depth (m)	Static level (m)	T (°C)	pH	EC ($\mu S\,cm^{-1}$)	Ca^{2+} ($mg\,L^{-1}$)	Mg^{2+}	Na^+	K^+	HCO_3^-	Cl^-	SO_4^{2-}	NO_3^-	TDS	$\delta^{18}O$ (‰ V-SMOW)	δ^2H	^3H (TU)	^{14}C (pmC)
1	Wealdian CI	350	80	45.6	21.7	7.74	5730	399.6	139.9	570.8	42.1	195.2	1298.2	878.2	0	4340	−7.4	−58	0.3 ± 0.3	
2	Wealdian CI	372	135	47.5	24.6	7.55	1963	169.3	57.2	234.8	32.3	189.1	385.5	377	7.1	1405	−7.5	−56	<0	
3	Wealdian CI	383	160	72.9		7.65	2601	234.1	66.4	300.2	42.5	176.9	547.2	534.5	0	1934	−8.2	−66		
4	Wealdian CI	338	124	38.7	23.1	7.62	1649	80.7	38.4	247.6	12.8	252.3	140.5	431.2	11.6	1104	−6.4	−40	1.14 ± 0.3	42.24 ± 0.21*
5	Wealdian CI	367	128	60	25	7.39	5040	310.1	163.2	771.3	0	213.5	685.9	1744.8	0	4036	−7.1	−52	0	
6	Wealdian CI	398	140	72		7.44	2840	245.3	68.0	331.5	25.9	195.2	583.2	608.3	1.9	2097	−8.1	−63		
7	Wealdian CI	366	98	49.53	24.4	7.45	1704	151.5	57.1	191.8	20.5	207.4	309.2	342.3	4.6	1245	−7.5	−51		
8	Wealdian CI	328	156	27.3	21.5	8.36	3124	293.1	91.8	300.2	43.7	164.7	823.4	548.2	0	2528	−8.0	−69	0	
9	Wealdian CI	312	85	26.8	23.6	8.01	2922	277.3	91.7	275.1	41.9	170.8	751.6	485.8	0	2269	−8.0	−66	0	
10	Wealdian CI	366	98		24.4	7.45	1704	142.5	57.6	149	19.5	207.4	344.2	279.7	0	1233	−7.7	−56		
11	Wealdian CI	337	102	43.75	22.1	7.83	6959	559.9	377.9	1063	39.8	317.2	1515.4	2657	0	6380	−5.8	−50	<0	
12	Wealdian CI	381	150	77	23.4	7.85	2165	175.8	79.5	211	24.2	201.3	476.3	413.1	0	1637	−7.6	−62	0.58 ± 0.3	
13	Wealdian CI	356	54	40	22.7	8.27	1247	109.2	46.7	101.4	14.1	189.1	151.0	283.3	0	867	−7.2	−45	0.3	72.2 ± 1.5
14	Wealdian CI	357	50		23.2	8.09	1731	95.2	55.7	158.5	18.9	189.1	304.0	283	8.1	1163	−7.7	−58	0	
15	Wealdian CI	317	50		23	7.79	9372	663.6	449.0	1571.8	68.5	237.9	3125.1	2127.9	0	8442	−6.4	−55	0	
16	Wealdian CI	323	40		24	7.61	2850	271.2	81.9	359.8	27.6	173	595.0	671.02	0	2123	−7.9	−64		
17	Wealdian CI	315	50	15	19.5	8.13	5613	519.1	203.5	555.3	51.5	176.9	1688.7	791.3	0	4411	−7.7	−66	0	24.2 ± 0.9
18	Wealdian CI	304	50		16	7.89	5950	523.6	319.2	1062.5	24.9	244	1248.2	2830.2	0	6715	−6.0	−47	0.6 ± 0.3	
19	Wealdian CI	307	20.8		19.5	7.94	1949	161.9	97.7	193.7	17.5	292.8	307.9	494.8	0	1543	−6.9	−48	0.1 ± 0.3	
20	Wealdian CI	327	50		20.6	7.98	4920	409.8	283.9	674.5	30.9	237.9	1002.7	1779.6	0	4541	−5.9	−46	0.6 ± 0.3	
21	Wealdian CI	341	40	30	21.8	8.29	1116	108.9	52.5	50.6	8.6	152.5	85.83	317.1	0	780	−5.6	−37	1.03 ± 0.3	68 ± 5
22	Wealdian CI	293	50	16	21	7.07	5400	575.1	153.2	525.8	86.5	237.9	947.1	1502.0	4	4032	−7.3	−60		
23	Albian CI	389	150		23.8	7.4	6400	325.5	169.5	784.4	23.6	176.9	976.8	1678.6	5	4140	−6.4	−46	0.3 ± 0.3	2 ± 0.1
24	Albian CI	391	150	70	22.3	8.28	1458	43.9	33.5	236.7	9.3	280.6	103.6	446.31	0.99	1075	−6.5	−43	0.4 ± 0.3	56.4 ± 1.8
25	Albian CI	390	126	78.9	25.2	7.6	2300	134.8	67.0	341.4	16.4	170.8	340.4	615.9	10.12	1614	−7.0	−45	0.05	
26	Albian CI	388			24.1	8.12	3691	101.8	205.5	601.9	13.7	219.6	694.6	1104.9	22	3080	−6.2	−43	0	
27	Albian CI	395	135		24.1	7.84	4449	355.2	102.3	683.5	0	207.4	805.8	1315.3	0	3592	−5.9	−40	0	
28	Albian CI	402	125		24.9	8.04	3770	250.8	127.8	603.4	0	213.5	594.2	1195	20.3	3157	−6.1	−43	0.5 ± 03	
29	ªSpring downstream	265				7.81	5940	444.1	196.2	746.4	91.2	237.9	1477.7	1066.7	30.1	4701	−6.8	−56		
	ᵇSpring upstream			NA		7.29	4510	432.5	141.3	476.8	55.6	146.4	1079	953	0	3284	−7.9	−58		

NA not accessible

* From Petersen (2014)

mineralization is being low to moderate for the majority (1163 to 2528 mg/l) with noticeably three more mineralized points No. 1 and 17 (with, respectively, 4340 and 4411 mg/l) and exceptionally the shallow well No. 15 with 8442 mg/l.

The second group of Na–SO$_4$ water type represented by 5 boreholes (No. 4, 5, 6, 7 and 11) and 4 shallow wells (No. 16, 18, 19 and 20). The mineralization for this group varies from 1104 to 4541 mg/l with relatively two more mineralized samples (No. 11 and 18 having, respectively, 6380 and 6715 mg/l).

The third group, Ca–SO$_4$ water type characterizes the less mineralized groundwater located in the recharge area. This facies is dominated by calcium and sulphate ions and represented by three shallow wells (No. 13, 21 and 22). The mineralization for the wells No. 21 and 13 is, respectively, 780 and 867 mg/l; however, the well No. 22 has a highly salinity of 4032 mg/l. This spatial variation of mineralization is illustrated in Fig. 5. From south to north, the following evolution is noticeable; the mineralization is low in southern study area, from Dehiba in the extreme south to El Asfer area with a variation from 867 to 2000 mg/l. Towards the north-west, an increase in the mineralization between the regions of Kambout and Oum ed Diab is observed, with a content from 2500 to 4700 mg/l. To the north, it decreases in the Douiret region in the well No. 21 having 780 mg/l. From northern Jebel Haddada up to Bani Khedach locality, high values of mineralization are observed varying from 4500 to 6700 mg/l. In the region of Ghomrassen, we note a low value in the well No. 19 equal to 1500 mg/l. This variation of the mineralization seems to result from the nature of the host rock of sandstone-type

dominated with clay and gypsum which is more important towards the north.

The presence of gypsum in sandstone deposits was recently demonstrated in different forms including large gypsified trunks up to 4 m long. Clay lenses on top of the sandstone beds are commonly rich in gypsum, and in some cases, some gypsified fossils have been documented (Fanti et al. 2012). These rich sand deposits in clay and gypsum, attributed to the top of the Douiret formation, are particularly well illustrated and exposed northern study area between the localities of Jebel Haddada and Oued El Khil where the EC measurements are the highest.

In order to thoroughly investigate the presence of these evaporitic facies, we referred to studies based on recent stratigraphic and paleontological data. The lower unit of the Douiret formation is interpreted as a tide-dominated coastal/deltaic plain characterized by relatively high marine ecosystems productivity. The overlying Douiret clay member is interpreted to represent deposition within a subsident, lagoonal system that was occasionally subject to major evaporitic conditions (Sabkha system) (Fanti et al. 2012). In southern Tataouine basin, particularly the region of kambout marks, the base of the Douiret formation juxtaposed to shallow-marine deposits of the Boulouha Formation. Noticeably, the highest values of mineralization were recorded in this region (Kambout). These interpretations explain the predominance of detected evaporitic facies as well as the spatial variability of groundwater mineralization in the study area.

The chemical facies of groundwaters from the upper Albian aquifer is quite uniform of Ca–SO$_4$ type with low to moderate electrical conductivities.

The water chemical composition upstream El-Achouch basin is of Na–Ca/Cl type with 4510 µS/cm. However, the analysed sample downstream El-Achouch spring (in Figs. 6, 7, 8, 9, 10, 11, 12) presents a chemical facies of Na–Cl type with 5940 µS/cm electrical conductivity. This relatively high conductivity is likely due to the change in the original chemical composition during the water transit in El-Achouch basin subjected to intensive evaporation effect.

In order to investigate the processes contributing to groundwater mineralization in Tataouine basin, plots of Na$^+$ versus Cl$^-$, Ca^{2+} versus SO$_4^{2-}$ and Ca^{2+} versus HCO$_3^-$ were established. The Na$^+$–Cl$^-$ relationship (Fig. 6a) has frequently been used to identify the mechanisms of acquiring groundwater salinity in arid and semiarid regions (Dixon and Chiswell 1992).

The majority of samples from the lower aquifer plot along the halite dissolution line (slope 1) or close to it. The depletion of Cl$^-$ contents relative to Na$^+$, observed for the samples from the Albian aquifer, is due to the cation exchange reactions releasing Na$^+$ at the expense of Ca^{2+} cations between groundwater and the clay fraction of the
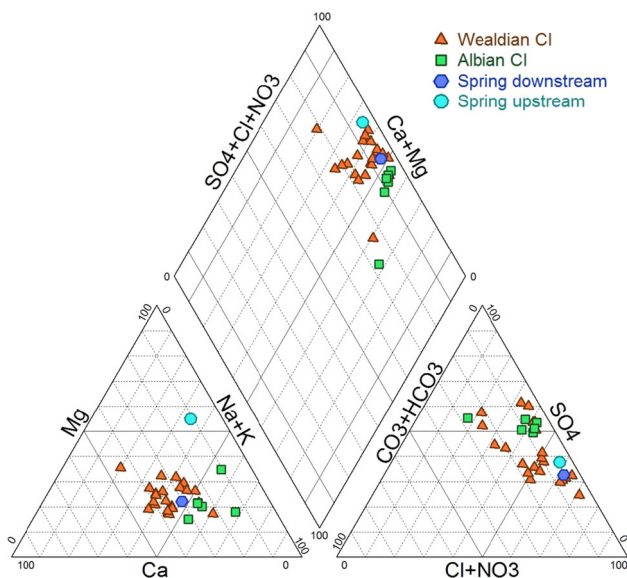
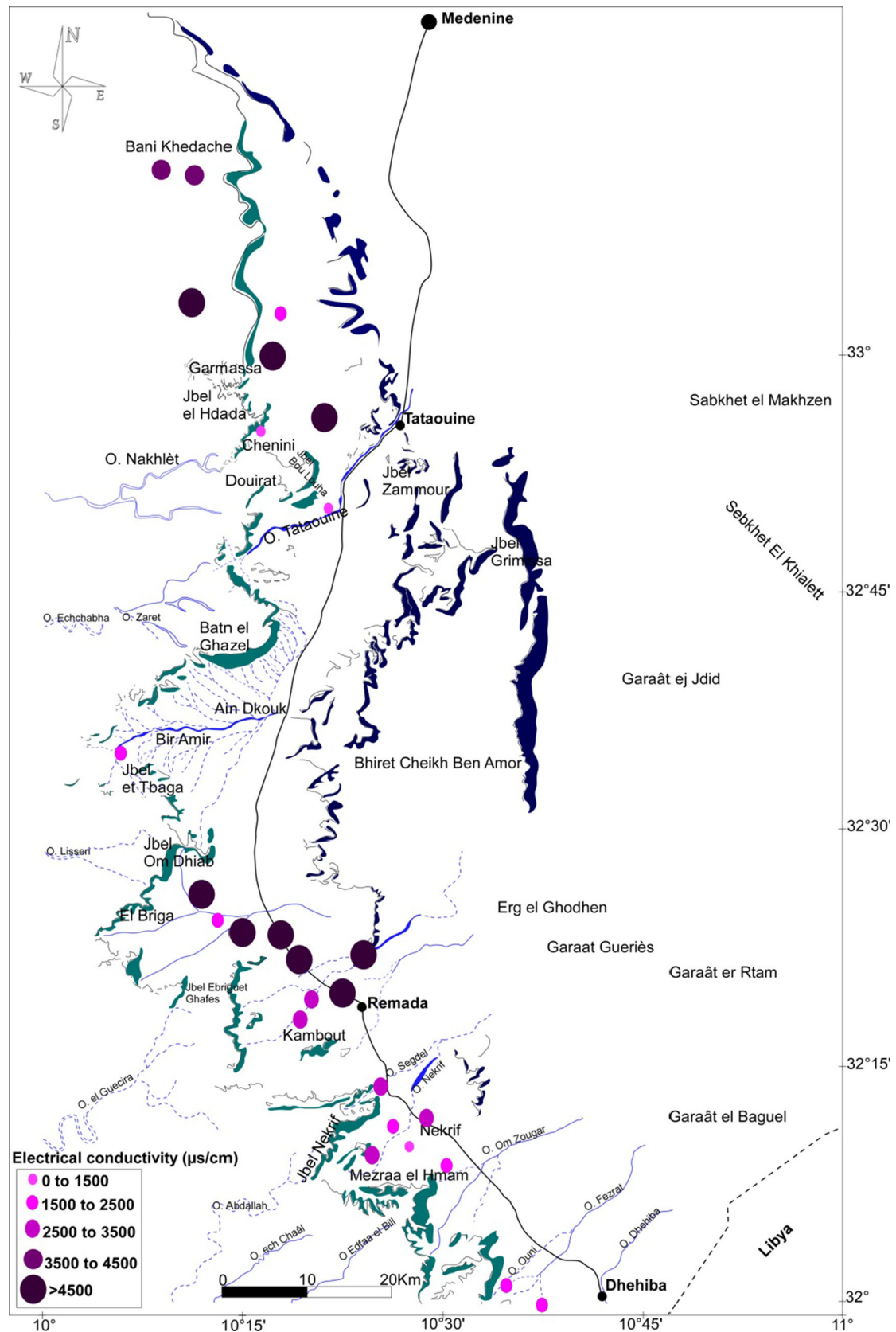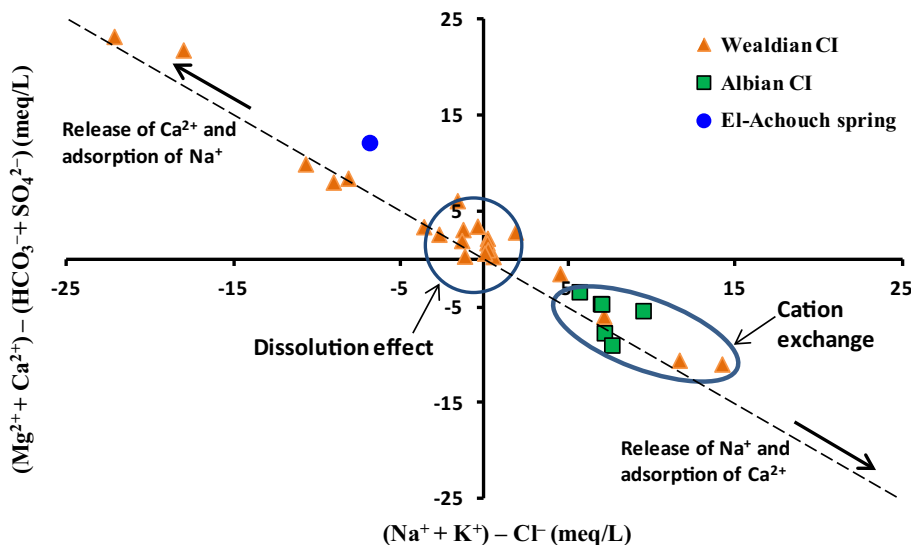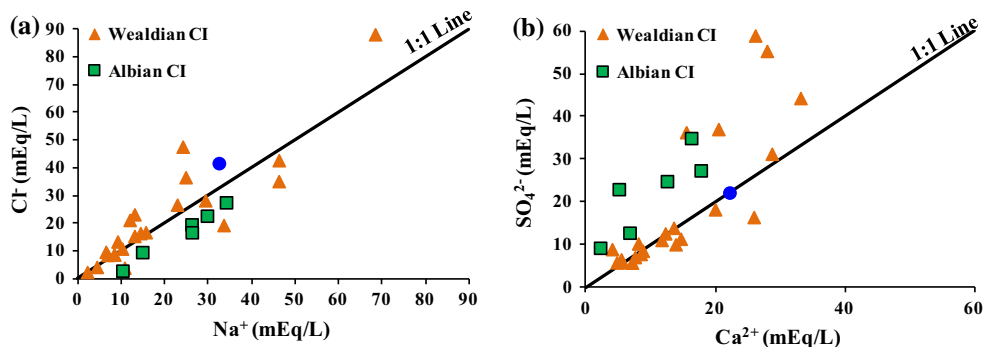**Fig. 4** Trilinear diagram showing the major chemical compositions of the CI-analysed water samples

Fig. 5 Spatial variability of the electrical conductivity in the study area

Fig. 6 Na$^+$ versus Cl$^-$ relationship (**a**) and Ca^{2+} versus SO$_4^{2-}$ relationship (**b**)

Fig. 7 Plots of [(Ca^{2+} + Mg^{2+}) − (SO$_4^{2-}$ + HCO$_3^-$)] versus [(Na$^+$ + K$^+$) − Cl$^-$] of the analysed water samples

aquifer material (Edmunds et al. 2003; Petalas and Lambrakis 2005). These samples which present molar [Na$^+$]/[Cl$^-$] ratios higher than 0.86 (theoric ratio of sea water) also exhibit a depletion of Ca^{2+} with respect to SO$_4^{2-}$ (Fig. 6b).

This is in good agreement with a Ca^{2+}–Na$^+$ cation exchange process leading to a softening of the water. This hypothesis could be justified by the relationship of (Ca^{2+} + Mg^{2+}) − (HCO$_3^-$ + SO$_4^{2-}$) versus (Na$^+$ + K$^+$ − Cl$^-$) (Garcia et al. 2001) in Fig. 7 which reveals that samples from the Albian aquifer are displaced towards positions that represent a gain in Na$^+$ and K$^+$ contents against a loss in Ca^{2+} and Mg^{2+} contents, supporting the hypothesis that the waters are involved in a cation exchange process. In the case of the absence of this phenomenon, all the points are positioned on the origin (Mc Lean et al. 2000).

This process does not seem contributed to the mineralization of most samples from Marbah El Asfer aquifer. Indeed, on the Ca^{2+} versus SO$_4^{2-}$ plot (Fig. 6b), we observe an excess of sulphates relative to calcium and which is not compensated by sodium ions. This probably

reflects the combined dissolution of gypsum and kieserite (Fig. 8) (MgSO$_4$–H$_2$O) disseminated in the CI lower aquifer (Wealdian).

The [Ca^{2+}]/[Mg^{2+}] ratio of these samples gives the lowest values among all groundwaters from Wealdian aquifer with values close to 1. These samples are also the most mineralized (from 4.04 to 6.71 g/l) and present the highest magnesium rates. It is likely that the dominance of evaporites in hosting rock is also related to further evolution of the evaporitic sequence; the kieserite in a marine environment being deposited after gypsum and halite.

The Ca^{2+} versus HCO$_3^{2-}$ relationship (Fig. 9) shows an excess of calcium for the majority of samples plotted below the calcite dissolution line 1:1 indicating therefore a presence of an alternate Ca source which could be the alternation and the erosion of gypsum and/or clay.

Samples which are very close to the calcite dissolution line reflect the dissolution of carbonatic minerals (likely the dolomite presented in this formation as mentioned in the geological part).

The HCO$_3^-$/(Cl$^-$ + SO$_4^{2-}$) (meq/l) versus electrical conductivity relationship (Fig. 10) indeed highlights

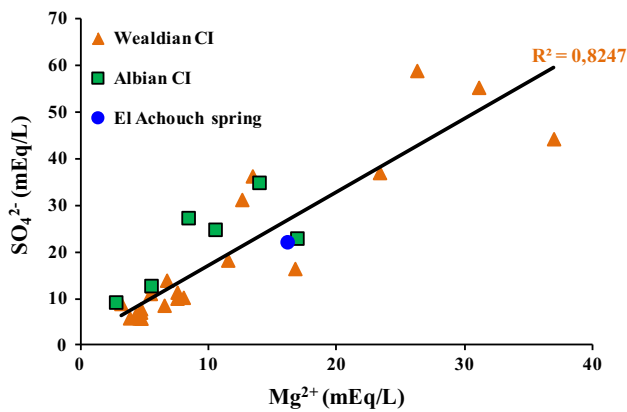**Fig. 8** SO_4^{2-} versus Mg^{2+} relationship

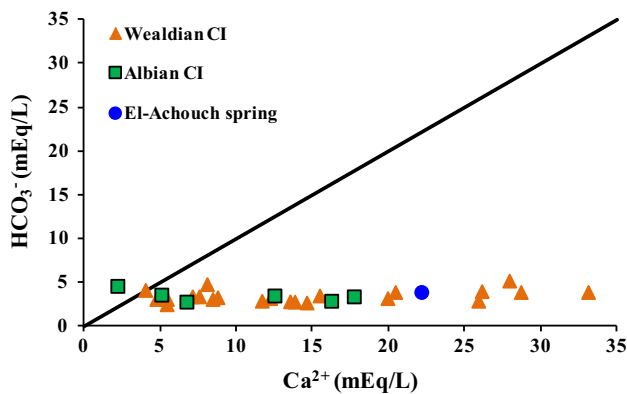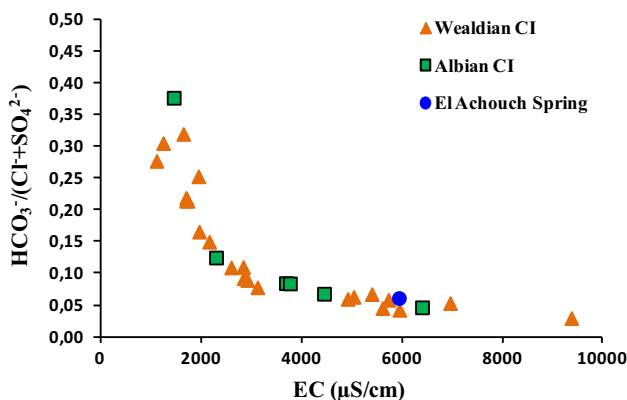**Fig. 9** HCO_3^- versus Ca^{2+} relationship

Fig. 10 Plot of HCO_3^- (Cl^- + SO_4^{2-}) (meq/l) versus electrical conductivity

prominently that the $HCO_3^-/(Cl^- + SO_4^{2-})$ ratio decreases gradually as well as the conductivity increases; for the lowest conductivities, the chemical acquisition results in the dissolution of minerals from the alteration of surrounding rocks and from the dissolution of sulphated and chlorinated evaporites included in the sedimentary sequence; however, for the highest conductivities, the

chemical acquisition of groundwaters results mainly in these evaporites dissolution which become the principal component of the aquifer sediments.

Such a process is illustrated in Fig. 11 showing the variation of groundwaters saturation indices which indicates an undersaturation state (SI < 0) with respect to evaporitic minerals such as gypsum, halite and anhydrite and a supersaturation for the majority of samples with respect to carbonatic minerals, revealing the presence of ionic exchange reactions significantly affecting groundwater composition.

Isotopic study

The stable isotope contents in CI groundwaters in the eastern piedmont of Dahar exhibit a wide range of variation between −8.2 and −5.6 ‰ versus V-SMOW for $\delta^{18}O$ and −37 and −69 ‰ versus V-SMOW for δ^2H. We have reported results on the δ^2H versus $\delta^{18}O$ diagram (Fig. 12) where we plotted the Sfax meteoric water line (SMWL) and the global meteoric water line (GMWL) defined by Craig (1961) ($\delta^2H = 8. \delta^{18}O + 10$). Considering only the highest rainfall events (>5 mm; rain without evaporation process under the cloud), the Sfax regional meteoric line obtained in the thermodynamic equilibrium conditions is equal to $\delta^2H = 8. \delta^{18}O + 13.5$ (Maliki 2000). The relatively high deuterium excess reflects the Mediterranean air masses vapour condensation. The weighted mean values of rainy events higher than 5 mm are equal to $\delta^{18}O = -4.6$ ‰ and $\delta^2H = -23.3$ ‰ (Celle-Jeanton et al. 2001).

Compared with current annual isotopic precipitation signatures of the nearest stations such as Sfax (−4.6 ‰ vs V-SMOW for ^{18}O for the period 2012–2013) and Kairouan (−4.5 ‰ vs V-SMOW from 2008 to 2012 weighted average), which present a relatively more humid climate between 220 and 270 mm of annual rainfall compared to Tataouine, only the most isotopically enriched points of the aquifer system could present a process of current recharge.

Some samples from the Wealdian aquifer are plotted near the meteoric lines and show contents significantly compared to those of recent precipitations with still a slight depletion. As mentioned above, this could be due to a mixing between recent rainfall and old residual water recharged under a different climate.

Samples from the upper Albian aquifer are located on or slightly below the world meteoric water line (a difference between 3 and 5 ‰ vs V-SMOW for δ^2H). This stable isotope enrichment suggests the contribution of the Albian sandstones outcrops to the actual recharge of the aquifer system through the infiltration of rainwater. However, because of the small amounts of the rainfall and their irregularities, inputs to groundwater remain relatively low.

Fig. 11 Plots of Calcite SI versus $(Ca^{2+} + HCO_3^-)$, Aragonite SI versus $(Ca^{2+} + HCO_3^-)$, Dolomite SI versus $(Ca^{2+} + HCO_3^- + Mg^{2+})$, Halite SI versus $(Na^+ + Cl^-)$, Anhydrite SI versus $(Ca^{2+} + SO_4^{2-})$ and Gypsum SI versus $(Ca^{2+} + SO_4^{2-})$, of the CI-analysed samples
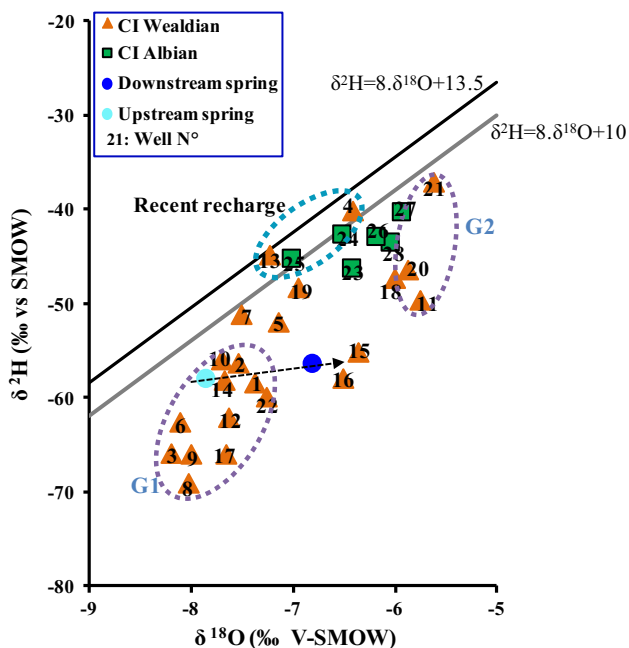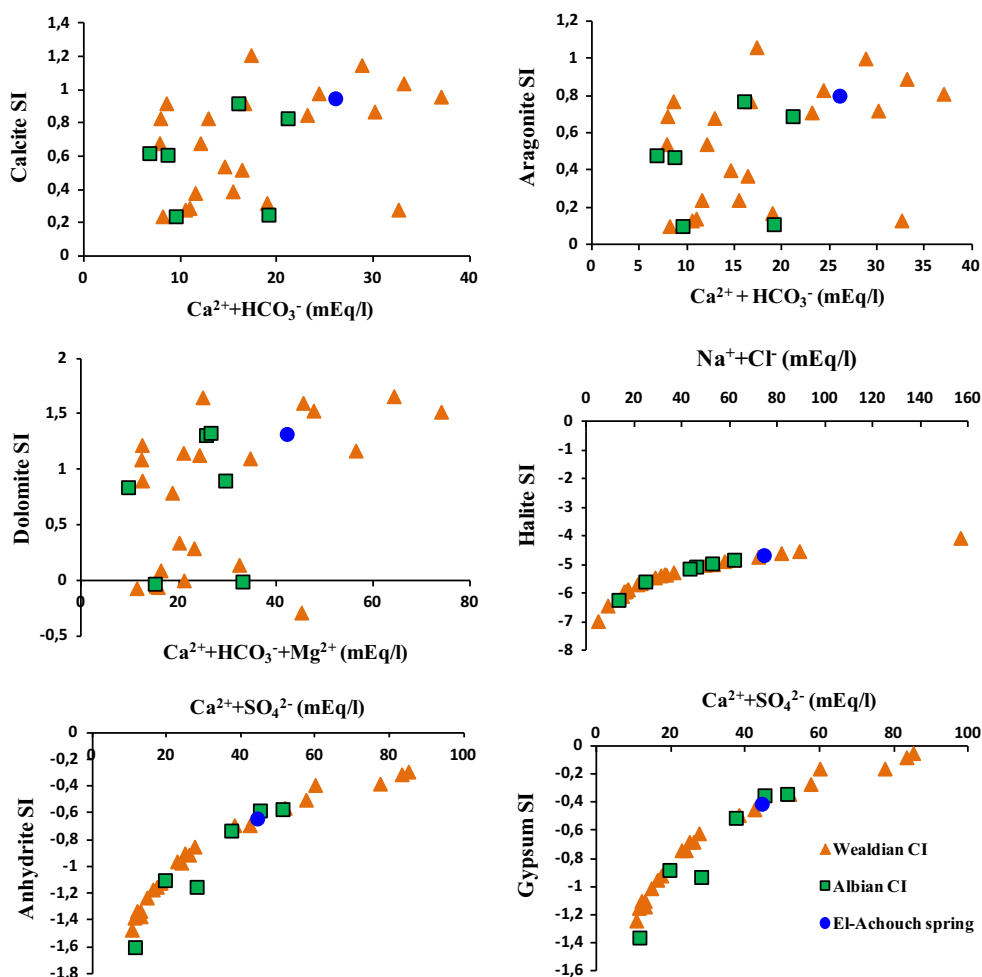
Fig. 12 Plots of δ^2H versus $\delta^{18}O$

In the ^{18}O versus ^{2}H diagram, the stable isotopes contents of samples from the lower Wealdian aquifer show a spatial variability over the study area (Fig. 12). We notice an enrichment in groundwater stable isotope contents from the south to the north (from −8.2 to −5.6 ‰ vs V-SMOW for $\delta^{18}O$). This distribution is represented mainly by two groups. The first group G1 represented by the most depleted samples Nos. 7, 12, 3, 2, 6, 14 and 16 located to the south of the region between Dehiba and Remada. The second group G2 represented by the most enriched samples Nos.17, 15, 5, 1, 4, 8, 9 and 22 located to northern Remada.

This spatial variability was explained with a statistical study of rainfall records from different stations throughout southern Tunisia over a period of 70 years. The study has shown that the spatial rainfall variability is related to longitude and seasonality than latitude and altitude (Ellouze et al. 2009), and this could be explained by the climate changes from a season to another and the irregularity of rainfall. In fact, the region receives a small amount of rainfall, which largely varies in time and space compared to northern and coastal regions. Also, southern Tunisia is

mainly a plane region, where rainfall variability is more governed by the Mediterranean Sea proximity, and shows more important contribution of present rainfall (more enriched than the paleorecharge) towards the north which could probably lead to this south–north isotopic enrichment gradient.

We notice on the ^2H versus ^{18}O diagram that El-Achouch spring and points nearby (No. 15 and 16) are located well below the GMWL. These points are characterized by low δ^2H values compared to others. The deuterium excess defined by d (‰) $\equiv \delta^2H - 8$. ^{18}O (Dansgaard 1964) is a useful indicator for the identification of secondary processes that influence the water isotopic composition ($\delta^{18}O$ and δ^2H) in the evaporation–condensation cycle. During precipitation and runoff, if the evaporation is low, the residual water shows no measurable change and generally keeps the $\delta^{18}O/\delta^2H$ signal that reflects its origin. However, if the water loss is important, the result is a noticeable change in the $d^{18}O$, d^2H water composition; this change becomes increasingly important as the disequilibria processes are important.

In our study, the "d" values vary between 5.8 and 11.2 ‰. Low values emphasize the predominance of the evaporation process during water infiltration as shown for evaporated surface water at El-Achouch spring downstream ($d = -1.8$ ‰). In the upstream of El-Achouch basin, the d excess is more elevated ($d = 5$ ‰) revealing the importance of this evaporation process during water shipment. The relatively high values of deuterium excess indicate rapid infiltration of rainwater and the absence of evaporation process. This parameter is highest for sample No. 4 (Mohsen Naili) which is located on the GMWL suggesting the presence of recent recharge as well as the well No. 21 (Salem Ben Salem Dabbabi) supplied by direct infiltration of rain water from the Tataouine wadi.

Points from the upper Albian level are characterized by relatively high deuterium excess (>8 ‰) compared to other samples from the lower aquifer especially points Nos. 24 and 25 with, respectively, 9.6 and 11 ‰. Conversely, the general conditions of the CI isotopic contents regionally indicate that these waters are plotted well below the actual meteoric water line; it is assumed that during the recharge period, the conditions of atmospheric circulations and the air masses origin were different to the present day resulting in an isotopic enrichment rather than a marked evaporation process (Edmunds et al. 2003).

The ^{18}O versus ^3H diagram (Fig. 13) identifies the possible sources of the aquifer recharge. The ^3H concentration measurements exhibit low values below the detection level for most samples indicating that groundwater residence time inside the aquifer is pre-1950. Analysis of some tritium samples show low values, below the level of detection for the most points; however, some shallow wells
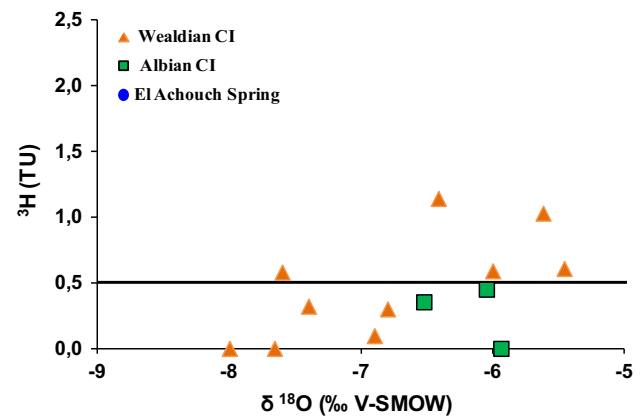

Fig. 13 ^3H versus ^{18}O relationship

from the Wealdian aquifer showed values of $^3H > 1$ TU. We can suppose that the origin of this component comes from recent precipitations on the CI outcrops in the eastern piedmont of Dahar or other processes such as recharge from river, as the well of Salem Ben Salem Dabbabi (Wealdian) which shows a tritium content of 1.03 UT, the weakest EC (1116 μS/cm), enriched stable isotope of −5.6 ‰ versus V-SMOW for oxygen 18 and which is close to the Tataouine wadi controlling its piezometric level.

To confirm the recent recharge process inferred from stable isotopes and tritium, we used the radiometric carbon-14 isotopes of the CI groundwaters. Three wells from the lower Wealdian aquifer (Nos. 13, 17 and 21) and two wells from the upper Albian aquifer have been analysed for ^{14}C measurements. The radiocarbon measurements revealed significant activities for some wells of the Wealdian aquifer hosted in Marbah el Asfer formation, particularly for the well No. 21 near the Tataouine wadi showing an activity >60 pmC of carbon 14 and a tritium concentration >1 TU as denoted above. This confirms the dominant role of this wadi in the aquifer recharge. Important ^{14}C activity is also recorded in wells Nos. 13 and 4 with, respectively, 72.2 and 42.2 pmC indicating the occurrence of recent recharge. Relatively, the lowest activity was measured in well No. 17 with 24.2 pmC.

For the upper Albian aquifer, the measured carbon-14 activity is low at borehole No. 23 (2 pmC) which could be due to the relatively high residence time of groundwater inside the aquifer. However, at borehole No. 24, the activity is more important (56.4 pmC); this relatively high activity reflects the contribution of the CI sandstones outcrops to the recent recharge of this aquifer.

The combination of isotopic tracers used in our study indicates the presence of two poles. A recent water pole isotopically enriched in stable isotopes and tritium contents and characterized by high ^{14}C activities as well and a second old water pole depleted in stable isotopes, tritium

and characterized by low ^{14}C activities. The groundwater evolution between these two poles could indicate a likely mixing of old and recent water from the CI aquifer.

Eventually, as perspective for our work, it seems important to suggest valuable solutions in order to improve the recharge rates in the aquifer. To increase this aquifer recharge and preserve the groundwater from overexploitation leading to continued decline of piezometric level, the artificial recharge process seems the valuable solution in our case. This technique consists in diverting water from extreme rainfall events or floods into local natural or artificial reservoirs allowing the infiltration into shallow aquifer and preventing the water seepage in saline depressions such as Sabkha system in our case. This method effectiveness is mainly controlled by the permeability of the rock across which water is infiltrated into the aquifer. Thus, the water spreading along the permeable sections of wadi beds in Tataouine basin remains the technique that works best. This method ensures up to 70 % of recharge water infiltration (Cary et al. 2013) and presents the best solution from economic and environmental perspectives.

In Tataouine basin, the climate is arid and characterized by irregular and scarce rainfall. The surface water resources are limited to flood flows, very irregular, occasionally very abundant but limited to seasonal events. Depending on the flow rate and the alluvial deposits permeability, often a small part of this water infiltrates during the flood, resulting in the increase in water table piezometric level, while high water volumes are lost in the depressions therefore draining a part of the potential reservoir (Mamou 1990).

Another efficient way of performing artificial recharge is the use of treated wastewater. This technique is based on letting treated sewage infiltration downwards the aquifer. This method benefit is to avoid diverting as much water from wadis or rivers; however, it requires specific systems to treat and distribute waste water. Therefore, artificial recharge remains the most viable solution and essential strategy to face groundwater overexploitation; although it remains challenging to distribute and treat waste water, it is possible to store water for the dry season.

Conclusion

The clayey-sandstone deposits of the Continental Intercalaire constitute the main aquifers in southern Tunisia. In the piedmont of Dahar, the CI groundwaters are logged in two main aquifers: the upper Albian and lower Wealdian separated by clay strata attributed to the Douiret formation dated of lower Aptian. The hydrochemical study shows the prevalence of three water types (Na–Cl, Na–SO$_4$ and Ca–SO$_4$) for groundwater sampled from the lower Wealdian

level and showing a large spatial variability of chemical facies. For the Albian water table, the chemical facies is homogeneous of Ca–SO$_4$ type. The variation in the groundwater total mineralization seems to result from the lithology of the hosting rock and mainly of evaporitic minerals. An isotopic approach was applied to study the possibility of a recent recharge of the CI water table in Dahar piedmont. Groundwater stable isotope (δ^{18}O, δ^{2}H) contents, from the lower Wealdian level ranging from -8.0 to -5.6 ‰ versus V-SMOW for oxygen 18 and from -69 to -37 ‰ versus V-SMOW for deuterium, demonstrate a noticeable enrichment from the south towards the north of the study area. Albian groundwater isotopic measurements (δ^{18}O, δ^{2}H) show relative enrichment suggesting the current contribution of the Albian sandstones outcrops in the aquifer recharge through rainwater direct infiltration. The deepest groundwater exhibits the most depleted values in heavy isotopes (-8.2 ‰ vs V-SMOW ^{18}O Mazraa Hmam well depth 160 m). Tritium analysis shows significant values for some shallow wells (>0.5 UT) which highlight the presence of recent recharge. This is consistent with the important radiocarbon activities assuring an obvious sign of recent recharge for some shallow waters of the CI aquifer in the eastern piedmont of Dahar area.

References

Abdallah H, Meister C (1997) The Cenomanian–Turonian boundary in the Gafsa-Chott area (southern part of central Tunisia): biostratigraphy, paleoenvironments. Cretac Res 18:197–236

Baba-Sy O (2005) Recharge et paléorecharge du Système Aquifère du Sahara Septentrional. Thèse de Doctorat, Université de Tunis El Manar, Tunisie, p 261

Barale G, Ouaja M (2002) La biodiversité végétale des gisements d'âge Jurassique supérieur–Crétacé inférieur de Merbah El Asfer (Sud-Tunisien). Cretac Res 23:707–737

Ben Baccar B (1982) Contribution à l'étude hydrogéologique de l'aquifère multicouche de Gabès Sud. Thèse de 3ème cycle, Université Paris Sud, Orsay France, p 116

Ben Ismail MH (1991) Les bassins mésozoïques (Trias à Aptien) du sud de la Tunisie: stratigraphie intégrée, caractéristiques géophysiques et évolution géodynamique. Thèse de Doctorat, Université de Tunis II, Tunisie, p 446

Ben Youssef M, Biely A, Kamoun Y, Zouari M (1985) L'Albien moyen supérieur à Knemiceras forme la base de la grande transgression crétacée au Tebaga de Medenine (Tunisie méridionale). C R Acad Sci II A 300:965–968

Bodin S, Petitpierre L, Wood J, Elkanouni I, Redfern J (2010) Timing of early tomid-cretaceous tectonic phases along North Africa: new insights from the Jeffara escarpment (Libya–Tunisia). J Afr Earth Sci 58:489–506

Bouaziz S, Buffetaut E, Ghanmi M, Jaeger JJ, Martin M, Mazin JM, Tong H (1988) Nouvelles découvertes de vertébrés fossiles dans l'Albien du Sud tunisien. Bull Soc Geol Fr 4:335–339

Burollet PF, Manderscheid G (1965) Le Crétacé Inférieur en Tunisie et en Libye. Colloque Crétacé Inférieur. Mémoire BRGM, Paris, pp 769–794

Busson G (1967) Le Mésozoïque saharien, première partie: l'Extrême Sud tunisien. Publ. Centre Rech. Zones arides (C.N.R.S.), Série Géologie, 8, p 185

Cary L, Casanova J, Gaaloul N, Guerrot C (2013) Combining boron isotopes and carbamazepine to trace sewage in salinized groundwater: a case study in Cap Bon, Tunisia. Appl Geochem 34:126–139

Celle-Jeanton H, Zouari K, Travi Y, Daoud A (2001) Caractérisation isotopique des pluies en Tunisie. Essai de typologie dans la région de Sfax. C R Acad Sci II A 33:625–631

Craig H (1961) Isotopic variations in meteoric waters. Science 133:1702–1703

Dansgaard W (1964) Stable isotopes in precipitation. Tellus 16:436–468

Dixon W, Chiswell B (1992) The use of hydrochemical sections to identify recharge areas and saline intrusions in alluvial aquifers, southeast Queensland, Australia. J Hydrol 135:259–274

Edmunds WM, Guendouz AH, Mamou A, Moula A, Shand P, Zouari K (2003) Groundwater evolution in the Continental Intercalaire aquifer of Southern Algeria and Tunisia: trace element and isotope indicators. Appl Geochem 18:805–822

Ellouze M, Azri C, Abida H (2009) Spatial variability of monthly and annual rainfall data over Southern Tunisia. Atmos Res 93:832–839

ERESS (1972) Etude des Ressources en Eau de Sahara Septentrional. La nappe du continental intercalaire. Modèle mathématique. Plaquette 2. Rapport final, UNESCO, p 122

Fanti F, Contessi M, Franchi F (2012) The "Continental Intercalaire" of southern Tunisia: stratigraphy, paleontology, and paleoecology. J Afr Earth Sci 73–74:1–23

Garcia MG, Hidalgo M del V, Blesa MA (2001) Geochemistry of groundwater in the alluvial plain of Tucuman province Argentina. Hydrogeol J 9:597–610

Geyh MA (2000) An overview of ^{14}C analysis in the study of the groundwater. Radiocarbon 42(1):99–114

Guendouz A, Moulla AS, Edmunds WM, Shand P, Poole J, Zouari K, Mamou A (1997) Palaeoclimatic information contained in groundwaters of the Grand Erg Oriental, N. Africa. In: Isotope Techniques in the Study of Past and Current Environmental Changes in the Hydrosphere and Atmosphere. IAEA, Vienna, pp 555–571

Guendouz A, Moulla AS, Edmunds WM, Zouari K, Shands P, Mamou A (2003) Hydrogeochemical and isotopic evolution of water in the complex terminal aquifer in Algerian Sahara. Hydrogeol J 11:483–495

Huneau F, Dakoure D, Celle-Jeanton H, Vitvar T, Ito M, Traore S, Compaore NF, Jirakova H, Le Coustumer P (2011) Flow pattern and residence time of groundwater within the south-eastern Taoudeni sedimentary basin (Burkina Faso, Mali). J Hydrol 409:423–439

Kamel S, Hamed Y, Chkir N, Zouari K (2007) The hydrogeochemical characterization of ground waters in Tunisian Chott's region. Environ Geol J 54:843–854

Lazzez M, Zouaghi T, Ben Youssef M (2008) Austrian phase on the northern African margin inferred from sequence stratigraphy and sedimentary records in southern Tunisia (Chotts and Djeffara areas). C R Geosci 340:543–552

Maduabuchi C, Faye S, Maloszewski P (2006) Isotope evidence of palaeorecharge and palaeoclimate in the deep confined aquifers of the Chad Basin, NE Nigeria. Sci Total Environ 370(2–3):467–479

Maliki MA (2000) Etude hydrogéologique, hydrochimique et isotopique du système aquifère de Sfax (Tunisie). Thèse de Doctorat, Université de Tunis II, Tunisie

Mamou A (1989) Les aménagements de conservation des eaux et des sols comme moyen de recharge des nappes du Sud tunisien. Direction générale des ressources en eau, Tunisie, p 23

Mamou A (1990) Caractéristiques, Evaluation, Gestion des ressources en eau du Sud Tunisien. Thèse de Doctorat d'Etat, Université de Paris Sud, Orsay France, p 426

Mc Lean W, Jankowski J, Lavitt N (2000) Groundwater quality and sustainability in alluvial aquifer, Australia. In: Sililoo O et al (eds) Groundwater, Past Achievement and Future Challenges. A Balkema, Rotterdamm, pp 567–573

OSS (2003) Système aquifère du Sahara septentrional: gestion commune d'un bassin transfrontière. Rapport de synthèse, Observatoire du Sahara et du Sahel, Tunisie, p 275

Penna D, Stenni B, Wrede S, Bogaard TA, Gobbi A, Borga M, Fischer BMC, Bonazza M, Charova Z (2010) On the reproducibility and repeatability of laser absorption spectroscopy measurements for δ^2H and $\delta^{18}O$ isotopic analysis. Hydrol Earth Syst Sci 7:2975–3014

Petalas C, Lambrakis N (2005) Simulation of intense salinization phenomena in coastal aquifers-the case of the coastal aquifers of Thrace. J Hydrol 324(1–4):51–64

Petersen J (2014) Traçage isotopique (^{36}Cl, ^4He, ^{234}U) et modélisation hydrogéologique du Système Aquifère du Sahara Septentrional Application à la recharge Quaternaire du Continental Intercalaire. Thèse de Doctorat, Université Aix Marseille, France, p 283

Peybernès B, Almeras Y, Ben Youssef M, Mello J, Rey J, Zargouni F (1985) Nouveaux éléments de datation dans le Jurassique du Sud Tunisien (Plateforme saharienne). C R Acad Sci II A 300:113–118

Raulin C, de Lamotte D, Bouaziz S, Khomsi S, Mouchot N, Ruiz G, Guilllocheau F (2011) Late Triassic–early Jurassic block tilting along E-W faults, in southern Tunisia: new interpretation of the Tebaga of Medenine. J Afr Earth Sci 61:94–104

Robaszynski F, Zagrarni MF, Caron M, Amédro F (2010) The global bio-events at the Cenomanian–Turonian transition in the reduced Bahloul Formation of Bou Ghanem (central Tunisia). Cretac Res 31:1–15

Teissier JL (1968) Alimentation en eau potable de la ville de Remada. Etude hydrogéologique préliminaire. Direction des resources en eau, Tunisie, p 12

Underdown R, Redfern J, Lisker F (2007) Constraining the burial history of the Ghadames Basin, North Africa: an integrated analysis using sonic velocities, vitrinite reflectance data and apatite fission track ages. Basin Res 19:557–578

Yahyaoui H (1996) Etude hydrogéologique des aquifères du piémont oriental et du flanc occidental du Dahar. Thèse de Doctorat, Université de Tunis El Manar, Tunisie, p 166